


**Chapter 4: Construction and performance  
assessment of Recirculating packed bed  
biofilm reactor (RPBBR) for effective  
biodegradation of *p*-cresol from wastewater**



The content that is included in this chapter has been published.

---

*Jaiswal, V.K., Sonwani, R.K., Singh, R.S., 2023. Construction and performance assessment of Recirculating packed bed biofilm reactor (RPBBR) for effective biodegradation of p-cresol from wastewater. Bioresour. Technol. 384, 129372. <https://doi.org/10.1016/j.biortech.2023.129372>*



#### 4.1. Introduction

The inorganic and organic pollutants released from industries such as chemicals, petrochemicals, coking plants, paper mills are considered as a severe concern worldwide (Tiwari et al., 2023). Among the various pollutants, phenolic compounds are generally found in various industrial effluents involved in the production of herbicides, coke ovens, and coal conversion operations (Jaiswal et al., 2023). Furthermore, it has been reported that the wastewater from some of these industries often released into the soil and contaminates nearby water supplies and agricultural fields (Panigrahy et al., 2020). The phenolic chemical 4-methyl phenol (*p*-cresol) is a natural substance found in crude oil, and human/animal urine (Gonzalez-Blanco et al., 2012). Severe exposure to phenolic compounds damages the heart, liver, kidney, and neurological system (Shim et al., 2019; Singh et al., 2022a). The phenolic compound is considered one of the “substances undesirable in excessive proportions” by the European Union (Xenofontos et al., 2016). The World Health Organization (WHO) has established a permissible limit of 0.001 mg L<sup>-1</sup> to regulate the amount of *p*-cresol compounds in drinking water (WHO, 1963). Therefore, the effluent containing phenolic compound must be treated to an adequate level before being discharged into open water bodies to prevent severe water pollution due to its toxicity. These pollutants are generally eliminated by electrolytic oxidation, catalytic oxidation, photocatalytic degradation, and adsorption (Mahdavianpour et al., 2018). However, these treatments are expensive and by-products formed during the process may be more toxic than the original pollutants (Martinkova et al., 2016). However, microbial remediation is favoured over conventional physicochemical techniques due to their environmental friendliness, cost-effectiveness, and the possibility of complete oxidation of the pollutants (Iliuta and Iliuta, 2022). Numerous microorganisms have been identified for degrading cresol and phenol from contaminated waste water. The microorganisms, such as *Pseudomonas citronellolis* NS1 (Panigrahy et al., 2020), *Pseudomonas sp.* (Hamitouche et al., 2016), *Chlorella vulgaris* (Xiao et al., 2019), *Pseudomonas putida* (Surkatti and El-Naas, 2014), *Advenella sp.* LVX (Xenofontos et al., 2016), *Rhodococcus*, *Achromobacter*, PSB-M 3, and *Sphingobium* (Ailijiang et al., 2021) have been investigated for the degradation of phenolic compounds. Usually, these bioremediation processes are carried out through two modes; (i) free cells and (ii) immobilized cells. The free cell system utilizes a suspension of microbial cells, whereas immobilized cells

refer to the microorganisms attached to porous support media. The free microbes have several disadvantages, such as losing microorganisms, toxic effects from high ambient concentrations and unpredictable microbial growth rates (Sonwani et al., 2019). The immobilization technology overcomes the disadvantages of the free cell system (Bao et al., 2021) by providing high removal efficiency of pollutants, chemical stability, and high biomass development in the face of adverse environmental circumstances (Maurya et al., 2022). Various researchers have observed that immobilizing the microbial cells in a suitable matrix can enhance the ability of microbial species to degrade organic pollutants during the bioremediation process (Shahabivand et al., 2022). The biodegradation of the phenolic compounds has been carried out in various attached growth bioreactors such as Packed Bed Bioreactors (PBBRS), Rotating Biological Contactors (RBCS), and Moving Bed Bio film reactors (MBBRs) (Swain et al., 2021). In attached growth bioreactors, the biodegradation process is greatly affected by the morphology, chemical constituents, and bioaffinity of the biocarriers. Therefore, in recent times, there has been significant interest in developing cost-effective, permeable, and durable biocarriers. Numerous carriers have been utilized to immobilize the microbes in this direction, including activated carbon (AC), sugarcane bagasse (SB), low-density polyethylene (LDPE), calcium alginate (CA), polyacrylamide, and polypropylene (PP), as well as polyurethane foam (PUF) (Ong et al., 2015). From the perspective of process engineering, PBBRs have numerous benefits, including high yield operation, convenience in scaling up, potential automation of separation processes leading to high degrees of purification, ability to treat large volumes of wastewater continuously by the specific number of immobilized cells, and the ability to reuse biomass (Banerjee and Ghoshal, 2016). Numerous studies have reported that immobilized cells in PBBRs can successfully biodegrade various harmful pollutants (Basak et al., 2019, Zhou and Nemati, 2018). Another benefit of PBBRs is the development of micro-niches with varying oxygen concentrations inside the supporting material's pores and within the layers of the biofilm (Martinkova et al., 2016). This study is focused on investigating the effects of process parameters such as, inoculum dose, pH of solution, and NaCl concentration on the specific growth of microbes. Furthermore, a comparative study of biodegradation of *p*-cresol was done in batch and continuous mode operation in RPBBR. Biodegradation kinetics was also evaluated. The effectiveness of RPBBR in terms of shock-loading of *p*-cresol and the metabolic pathway of the degraded sample were investigated. The bacterial toxicity assessment of the degraded products was also carried out.

## 4.2. Chemicals and methods

### 4.2.1. Mineral salt medium (MSM) and chemicals

In this present study, *p*-cresol (99%) and MSM (Mineral salt medium) were prepared as per the methods given in **Chapter 3 (Section 3.2.1)** in detail. Acclimatization, isolation and identification of *p*-cresol degrading pure strain have been discussed in previous studies ([Jaiswal et al., 2023](#)). Bacterial consortia (*Serratia marcescens* strain HL 1 and *Ochrobactrum intermedium* VrB9) were used in the biodegradation of *p*-cresol. The details of bacterial consortia have been discussed in the Appendix (**Appendix 4 (a)**).

### 4.2.2. Analytical methods

The concentration of bacterial cells and residual-cresol concentration were analysed as per the details given in **Chapter 3 (Section 3.2.4)**. Scanning electron microscopy (SEM) (Nova SEM 450, FEI, USA (S.E.A.) Pvt. Ltd., Singapore) was used after 15 days to evaluate the morphological characterization of the PUF carrier. GC–MS analysis employed (GC 7890B, 5977B GC/MSD) with HP- 5 MS column (30 m × 0.25 mm × 0.25 μm) containing FID detector and helium as carrier gas was used to perform the GC–MS analysis. The bioluminescence intensities of the treated, untreated, and control water samples were measured using a Horiba Fluorescence spectrophotometer (Model No.: PTI Quanta master TM 8000 series).

### 4.2.3. Process optimization for biodegradation of *p*-cresol

The process parameters, such as inoculum dose, pH, and NaCl concentration were optimized to enhance the specific growth and biodegradation of *p*-cresol. The inoculum of 2, 4, 6, 8, 10, 12, 14 and 16 (mL/100 mL) was varied. The optimum pH was determined by conducting experiments at various pH values (5, 6, 7, 8 and 9). The %NaCl was varied from 0.2 to 1.2 (w/100 mL). All the experiments were conducted at laboratory condition. The samples were collected at regular intervals to monitor bacterial growth.

### 4.2.4. Recirculating packed bed biofilm reactor

Recirculating packed bed biofilm reactor (RPBBR) was fabricated of borosilicate glass with a height of 60 cm and inner diameter of 5.5 cm, having a working capacity of approximately 1.2 L. Pre-sterilized PUF (1 cm × 1 cm × 1 cm) was used as the carrier for immobilization of bacterial

consortium due to its high porosity with strong resistance to water adsorption (Moghaddam et al., 2019). RPBBR was run for 15 days in batch mode. MSM as nutrient and *p*-cresol ( $50 \text{ mg L}^{-1}$  to  $100 \text{ mg L}^{-1}$ ) as carbon source were used under aerobic condition for the formation of biofilm on the carriers. A comparative study in batch mode has also been carried out with various concentrations of *p*-cresol ( $100 \text{ mg L}^{-1}$  to  $500 \text{ mg L}^{-1}$ ). All experiments were performed in triplicate. The constant volumetric flow rate of air ( $1 \text{ L min}^{-1}$ ) was maintained using rotameter (Flow point, India). A peristaltic pump (ELECTROLAB, PP- 50 V) was used to supply *p*-cresol solution at various flow rates to the reactor. pH and dissolved oxygen (DO) within the reactor was measured using pH meter (HD 2305.0; Delta OHM; Italy) and DO meter (HD 2109.1; Delta OHM; Italy) (Fig. 4.1.), respectively. The experiments were performed under laboratory condition.

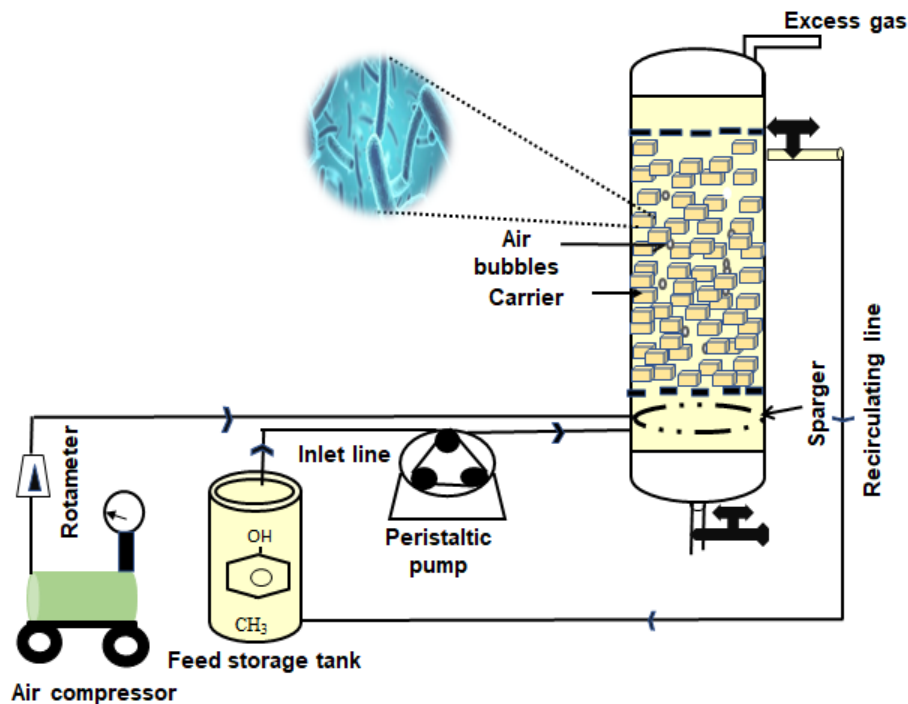


Fig. 4.1. Systematic diagram of recirculating packed bed biofilm reactor

#### 4.2.5. Biodegradation kinetic model for *p*-cresol

The first-order kinetic model, Eq. (4.1) can be describe the biodegradation kinetics of hydrocarbons (Sharma and Pandey, 2022)

$$\frac{dc}{dt} = k_p \times C \dots \dots \dots (4.1)$$

Integrating **Eq. (4.1)**

$$\ln \frac{C_0}{C} = k_p \times t \dots \dots \dots (4.2)$$

where  $k_p$  is first-order degradation constant,  $C_0$  is the initial concentration of *p*-cresol and  $C$  is the concentration of *p*-cresol at any time  $t = t$

Biodegradation of *p*-cresol half-life calculated by using **Eq. (4.3)**

$$\frac{t_1}{2} = \frac{0.69321}{k_p} \dots \dots \dots (4.3)$$

#### 4.2.6. Identification of intermediate by-product using GC–MS technique

Biodegraded *p*-cresol was centrifuged (RM-12C BL) at 10,000 rpm for 10 min. The supernatant obtained after centrifugation was filtered using a 0.45 μm Whatman filter paper to remove the remaining cellular debris. Ethyl acetate was used to extract the metabolites after the supernatant was acidified (pH 2 with 0.5 M H<sub>2</sub>SO<sub>4</sub>) (Panigrahy et al. 2020). The metabolites of biodegraded *p*-cresol were extracted using ethyl acetate and followed by removing moisture in a rotary vacuum evaporator (IKA RV 10). The samples were diluted in chloromethane and used for GC–MS analysis. The temperature of the injector was kept between 25 °C and 300 °C. Injection of samples into the GC–MS was done at the split ratio 5:1.

#### 4.2.7. Growth kinetics for biodegradation of *p*-cresol and bacterial toxicity assessment

The bacterial growth kinetics were analysed as per the details given in **Chapter 3 (Section 3.2.5)**. The bacterial toxicity of treated, untreated, and controlled sample were analysed as per the details given in **Chapter 3 (Section 3.3.6)**

### 4.3. Results and discussion

#### 4.3.1. Biodegradation activity of single and consortium strain

*p*-Cresol degrading strains were isolated from the enriched sample using an enrichment approach. The two best *p*-cresol degrading strains were selected and used for consortium development based on their percentage removal efficiency of *p*-cresol (**Appendix 4 (b)**). It was observed that the percentage removal of the bacterial consortium was higher than the individual strain under the same condition (**Appendix 4 (b) Table 4 A**).

### 4.3.2. Effects of inoculum dose on specific growth

A sufficient amount of inoculum is necessary to reduce the period of the lag phase, accelerate the degradation rate, and initiate the exponential growth phase. The effect of inoculum dose on specific growth was illustrated in **Fig. 4.2.(a)**. The specific growth of microbes continuously increases ( $0.04 \pm 0.0061 \text{ h}^{-1}$  to  $0.16 \pm 0.00502 \text{ h}^{-1}$ ) with an increase in inoculum dose (2 mL to 14 mL). Maximum growth ( $0.16 \pm 0.0052 \text{ h}^{-1}$ ) was evaluated at 14 mL of inoculum dose. However, with a further increase in inoculum dose (16 mL), the specific growth slightly decreases ( $0.16 \pm 0.0052 \text{ h}^{-1}$  to  $0.15 \pm 0.0024 \text{ h}^{-1}$ ). The decrease in specific growth might be due to decreased dissolved oxygen and increased competition for nutrients ([Singh et al., 2022b](#)).

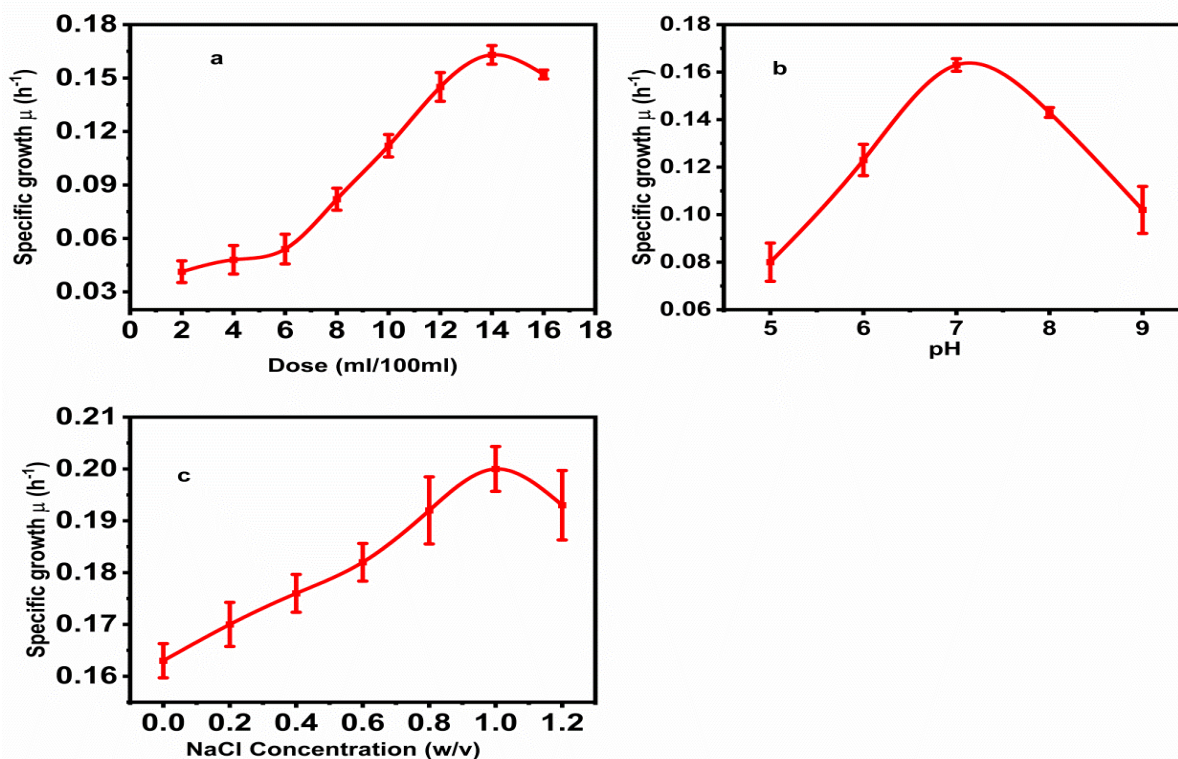


**Fig. 4.2.** Effect of bacterial consortia dose (a), pH (b), NaCl concentration (w/100mL), and (c) on specific growth of *p*-cresol biodegradation ( $100 \text{ mg L}^{-1}$ )

According to [Sarkar and Dey \(2020\)](#), increasing the inoculum dose reduces the lag period and accelerates biodegradation. Hence, 14 mL was the optimal inoculum dose for *p*-cresol biodegradation. High inoculant doses may alter bacterial features that affect the pollutant degradation rate ([Yang et al., 2017](#)). Furthermore, a higher inoculum dose ( $>14 \text{ mL}$ ) inhibited the microbial growth, which could be attributed to a decrease in dissolved oxygen and increased

competition for available resources (Eltoukhy et al., 2020). Xu et al. (2021) investigated the effects of inoculum dose (2%, 5%, 8%, 10%, 12% and 15%) on the biodegradation of phenol (500 mg L<sup>-1</sup>) using the *Acinetobacter lwoffii* NL1 strain. Their finding shows that as the dose increases from 2% to 10%, the time required for phenol degradation decreased (20 h to 14 h). The results were attributed to an increase in inoculum dose, which accelerated the transition of bacteria into the exponential growth phase by shortening the lag phase.

#### 4.3.3. Effects of pH on specific growth

pH is one of the primary elements affecting microbial growth and enzyme activity. Most of the enzymes of neutrophilic organisms tend to denature under severe pH and lose catalytic activity conditions (Bera et al., 2017). As a result, metabolic activities are inhibited, resulting in the instant death of biomass (Bera et al., 2017). An optimal pH is crucial for bacterial cells to consume the pollutant effectively. Fig. 4.2.(b) shows the variation in the specific growth of microorganisms according to different pH values. The maximum specific growth ( $0.163 \pm 0.052 \text{ h}^{-1}$ ) of microorganisms was found at pH 7. This suggests that the strain is a neutrophilic bacterium. Extreme pH can cause enzyme denaturation and loss of catalytic activity (Bera et al., 2019). An optimal starting pH must be maintained to successfully utilize *p*-cresol or any nutritional source. Hence pH 7 is optimal for the maximum specific growth of microorganisms.

#### 4.3.4. Effects of NaCl concentration on specific growth

The effect of NaCl on the specific growth of microorganisms is illustrated in Fig. 4.2.(c). As the concentration of NaCl increases (0% to 1%), specific growth increases ( $0.163 \text{ h}^{-1} \pm 0.0052$  to  $0.20 \pm 0.0032 \text{ h}^{-1}$ ) and found maximum at 1% of NaCl (w/ 100 mL). Furthermore, an increase in the concentration of NaCl from 1% to 1.2% leads to slightly decreased growth rate ( $0.20 \pm 0.0032 \text{ h}^{-1}$  to  $0.19 \pm 0.0067 \text{ h}^{-1}$ ). Higher specific growth at low amounts of NaCl ( $\leq 1 \text{ g}/100 \text{ mL}$ ) may be due to bacterial growth enhanced by a small amount of NaCl supplement. However, the decrease in specific growth suggested that microbial species might be stressed under high NaCl concentration, which reduces cellular activity (Jiang et al., 2017). Another study suggested that increased NaCl concentration above the optimal value may cause reduced bacterial metabolic activity that directly affects the growth of microorganisms due to plasmolysis, thus adversely affecting microbial activity (Li et al., 2019). According to Afzal et al. (2007), it has been

observed that a halophilic bacterial strain *Halomonas sp.* was able to degrade phenol present in saline industrial wastewater containing various concentrations (1% to 14% by weight) of sodium chloride. The study revealed that the most effective degradation of phenol occurred at an optimum concentration of 5% NaCl by weight.

#### 4.3.5. Morphological analysis of packing material

Process variables such as pH, nutrition availability, substrate concentration, etc., affect how a biofilm develops on the medium (Sonwani et al., 2019). The metabolic activity of the bacteria and its extracellular compound are both necessary for the development of biofilm on the surface of the carrier (Wang et al., 2018). SEM (Appendix 4 (c)) study of the carrier before bacterial immobilization (0<sup>th</sup> day) confirmed the presence of micro-pores on the surface. After 15<sup>th</sup> days, micro-pores were occupied microorganisms, a sign of biofilm forming on the carrier surface. The formation of thick bacterial biofilm on the surface and pores of PUF demonstrates the effective colonization of bacterial cells on carriers.

#### 4.4. Comparative study of biodegradation of *p*-cresol in batch and continuous mode operation

The comparative study of biodegradation of *p*-cresol in batch and continuous mode operation was shown in Fig. 4.3. The removal efficiency continuously decreased ( $90.73 \pm 1.61\%$  to  $64.21 \pm 1.87\%$ ) as concentration increased ( $100 \text{ mg L}^{-1}$  to  $500 \text{ mg L}^{-1}$ ) in the batch mode operation. This decrease in % removal efficiency may be due to different inhibitory action of pollutants. Bera et al. (2019) utilized *Stenotrophomonas sp.* obtained from petroleum refinery wastewater for biodegradation of *p*-cresol and reported that  $400 \text{ mg L}^{-1}$  completely degraded within 189 h. The result reveals that the substrate consumption rate reduced with an increase in the initial concentration and resulted in a lowering of biodegradation due to the enhancement of *p*-cresol concentrations' inhibitory action. Furthermore, the performance of RPBBR was studied in continuous mode at fixed flow rate ( $2 \text{ mL min}^{-1}$ ). The removal efficiency of the continuous mode operation was  $99.36 \pm 02\%$  at  $100 \text{ mg L}^{-1}$  *p*-cresol. That is higher than the % removal in batch mode operation ( $100 \text{ mg L}^{-1}$ ). It is possible that effective mixing led to less mass transfer resistance, which is the cause of this improved degradation (Talha et al., 2018). The biodegradation process is high at low concentrations of *p*-cresol due to a fast sorption phase

caused by the physical-chemical interaction between the molecules and microbial cells wall (Surkatti and El-Naas, 2014). Meanwhile, further increase in the concentration of *p*-cresol (200 mg L<sup>-1</sup> to 500 mg L<sup>-1</sup>) % removal continuously decreased (91.91±1.91% to 71.38±1.87%), probably due to substrate inhibition. However, as substrate concentration increases, more time will be required for complete degradation (Swain et al., 2021). Similar results were obtained by Singh et al. (2008), who found how *Gliomastix indicus* degraded throughout a broad range of initial *p*-cresol concentrations (10 mg L<sup>-1</sup> to 700 mg L<sup>-1</sup>). They observed that as the initial concentration increased, the substrate consumption rate decreased because the substrate *p*-cresol increased the amount of inhibition.

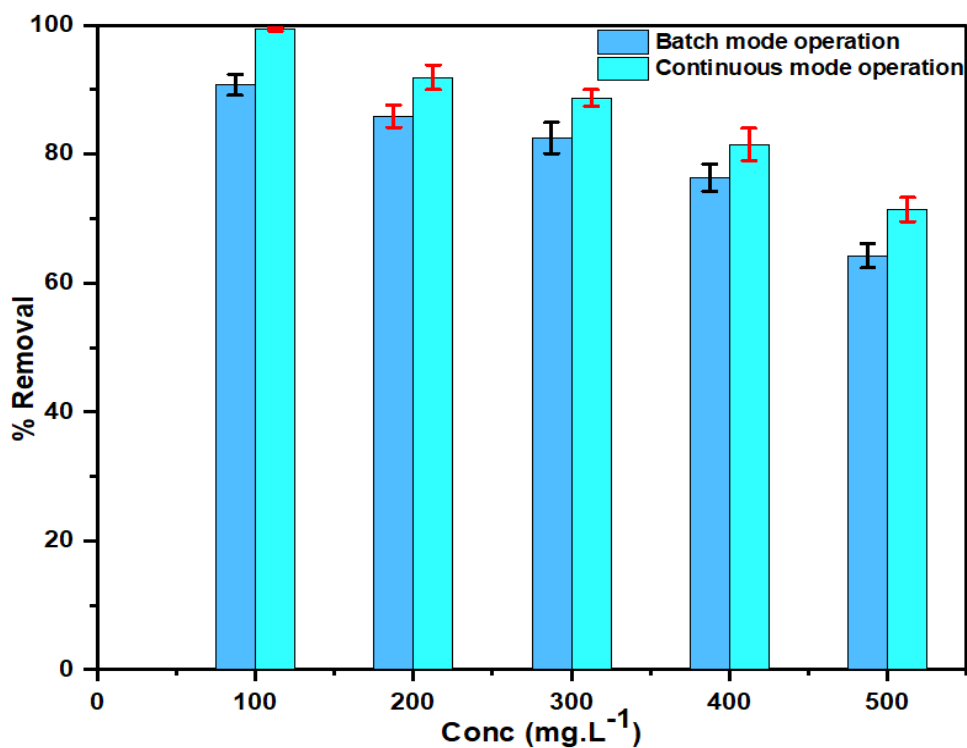


**Fig. 4.3. Comparative study of biodegradation of *p*-cresol in batch and continuous mode operations for various *p*-cresol initial concentrations**

#### 4.4.1. First-order biodegradation kinetics

It assumed that the degradation kinetics relied on the degradation rate constant  $k_p$  and the amount of active biomass. The amount of active heterotrophic biomass was expected to remain consistent throughout the experiment (Majewsky et al., 2011). The detailed first-order kinetics is illustrated in **Table 4.1** at optimized conditions.

**Table 4.1 Summary of first-order rate constant and half-life for biodegradation of *p*-cresol**

Initial concentration of <i>p</i> -cresol (mg L <sup>-1</sup> )	$\ln \frac{c}{c_0}$ vs $t$	Rate constant $k_p$ (day <sup>-1</sup> )	$t_{\frac{1}{2}}$ (day) $0.6932/(k)$	$R^2$
<b>Batch mode operation</b>				
100	$\ln \frac{c}{c_0} = 0.70t$	0.7086	0.97	0.9884
200	$\ln \frac{c}{c_0} = 0.63t$	0.6328	1.095	0.9653
300	$\ln \frac{c}{c_0} = 0.51t$	0.5151	1.345	0.9594
400	$\ln \frac{c}{c_0} = 0.38t$	0.3858	1.796	0.9537
500	$\ln \frac{c}{c_0} = 0.31t$	0.3129	2.215	0.9487
<b>Continuous mode operation</b>				
100	$\ln \frac{c}{c_0} = 0.96t$	0.962	0.72	0.9818
200	$\ln \frac{c}{c_0} = 0.73t$	0.7383	0.938	0.975
300	$\ln \frac{c}{c_0} = 0.72t$	0.7208	0.96	0.9783
400	$\ln \frac{c}{c_0} = 0.52t$	0.5281	1.31	0.9346
500	$\ln \frac{c}{c_0} = 0.40t$	0.4093	1.69	0.9915

This experiment was carried out with increasing concentrations of *p*-cresol (100 mg L<sup>-1</sup> to 500 mg L<sup>-1</sup>) in batch and continuous mode operation. It was observed that *p*-cresol concentration affected the rate constant in batch and continuous medium operations. The maximum rate constant value for batch and continuous medium operation was 0.70 day<sup>-1</sup> and 0.96 day<sup>-1</sup>, respectively, for the initial 100 mg L<sup>-1</sup> of *p*-cresol concentration. As concentration increased, the rate constant constantly decreased; consequently, the half-life increases. The decreased constant rate was due to the toxic effect of *p*-cresol. [Tepe and Dursun, \(2008\)](#) used *Ralstonia eutropha* for the biodegradation of phenol in batch-stirred and packed bed reactor with the assumption of first-order biodegradation kinetics, observed biodegradation rate constant was estimated at various flow rates. They found that the reaction rate decreases with the increased initial phenol concentration in both reactors and the maximum rate constant found in a continuous packed bed reactor.

#### 4.4.2. Impact of shock loading of *p*-cresol on the performance of the RPBBR

The continuous operation of RPBBR is necessary for real operation. Effect of shock loading (different *p*-cresol concentration from 500 mg L<sup>-1</sup> to 700 mg L<sup>-1</sup>) and flow rate (5 mL min<sup>-1</sup> to 55 mL min<sup>-1</sup>) at fixed Retention time ((RT) =1 day) is demonstrated in Fig. 4.4.

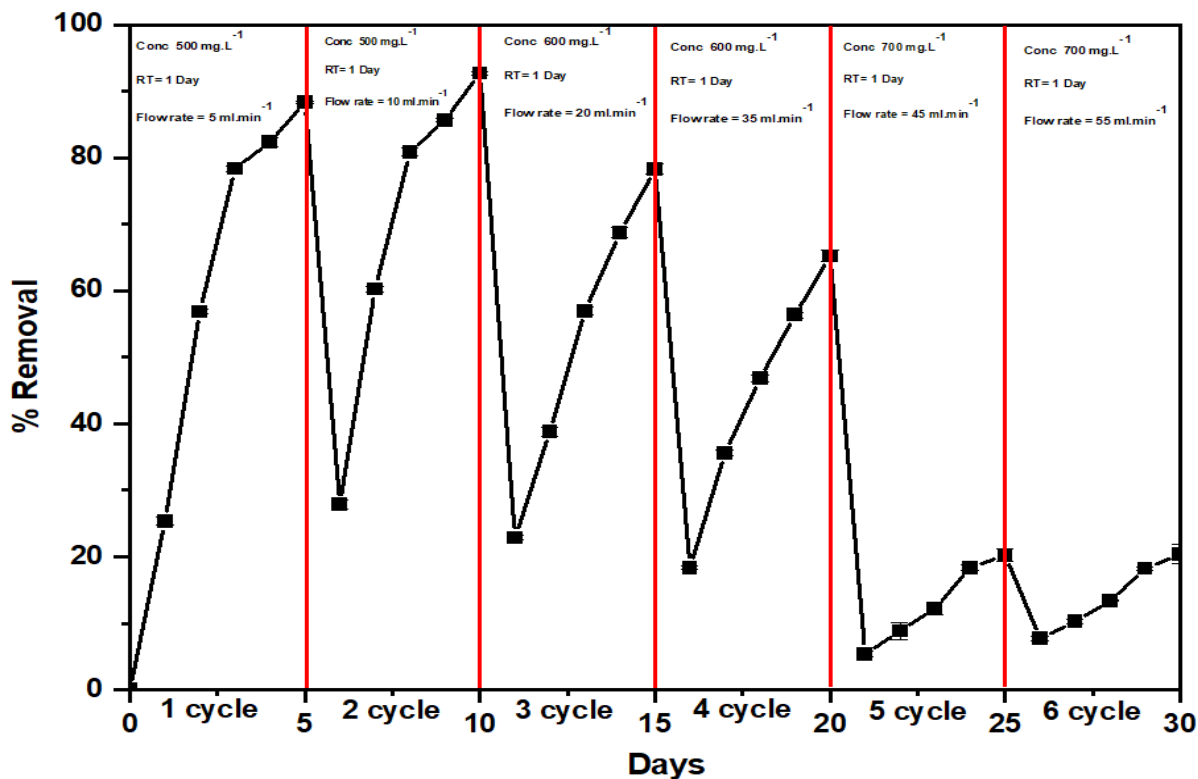


Fig. 4.4. Effect of shock disturbance on the performance of RPBBR for biodegradation of various concentrations of *p*-cresol and flow rate at constant retention time

The shock-loading operation included the six-cycle operating phases. The removal of *p*-cresol was influenced by both the flow rate and initial *p*-cresol concentrations. As flow rate increased from 5 mL min<sup>-1</sup> to 10 mL min<sup>-1</sup>, the removal efficiency increased from 88.38% to 92.72%, respectively after 1<sup>st</sup> cycle and initial concentration of 500 mg L<sup>-1</sup>. However, the removal efficiency was decreased with increasing flow rate from 20 mL min<sup>-1</sup> to 35 mL min<sup>-1</sup> at initial concentration of 600 mg L<sup>-1</sup>. The performance of continuous bioreactor negatively affected against the high loading rate (Oberoi and Philip, 2017). The high flow rate led to the loss of more biomass and subsequently reduced the biodegradation efficacy (Surkatti and El-Naas, 2014). Similar kinds of effect were noticed for biodegradation Acid blue 113 dyes in fixed bed reactor by Tiwari et al. (2022).

### 4.4.3. FTIR analysis GC–MS analysis of biodegraded *p*-cresol

#### 4.4.3.1. FTIR analysis of biodegraded *p*-cresol

The FTIR spectrum of biodegraded *p*-cresol solution was analyzed in the range of wave number 4000  $\text{cm}^{-1}$  to 500  $\text{cm}^{-1}$  (**Appendix 4 (d)**). The spectra at 3440  $\text{cm}^{-1}$  reveals O-H shifting ([He et al., 2021](#)). The peak at 2979  $\text{cm}^{-1}$  attributed to the presence of the methyl group. Similar findings relating to the existence of methyl group at wave number 2977-2979  $\text{cm}^{-1}$  have been reported ([Panigrahy et al., 2020](#)). The band between 1700-1630  $\text{cm}^{-1}$  is characterized by conjugate C=O and deconjugate C=O vibrations with aromatic or C=C elements ([Zghari et al., 2017](#)). The peak revealed the presence of methyl-substituted benzene derivatives detected at wave number 1385  $\text{cm}^{-1}$ . This is strongly confirmed by the reported literature, which states that methyl-substituted benzene derivatives typically emerge in the 1415-1370  $\text{cm}^{-1}$  range ([Mathammal et al., 2016](#)). The spectra that emerged at 1270  $\text{cm}^{-1}$  and 1000  $\text{cm}^{-1}$  revealed the existence of the C–O–C group. Similar trends for the presence of the C-O-C group have been reported for absorption spectra of 1260  $\text{cm}^{-1}$  and 1080  $\text{cm}^{-1}$  ([Panigrahy et al., 2020](#)).

#### 4.4.3.2. Assessment of *p*-cresol biodegraded metabolic by-product using the GC-MS analysis

Several intermediate compounds closely connected to the biodegradation of *p*-cresol have been identified using GC–MS analysis. The mass spectra of the biodegradation of *p*-cresol comprised several fragmentation peaks (**Appendix 4 (e)**). The mass spectra obtained at  $m/z$  value of 125.0 demonstrated that the biodegraded product contained 4-methyl catechol ([Panigrahy et al., 2020](#)). However, a molecular ion peak at  $m/z$  116.0 indicated maleic acid production. The presence of maleic acid at 116.0  $m/z$  was also reported by [Zakaria et al. \(2020\)](#) during phenol degradation. Fragmented ion peak at 61.0  $m/z$  supported glycerol synthesis in the *p*-cresol biodegradation pathway. The metabolic products involved in the biodegradation of *p*-cresol could not be identified in the current investigation, especially those at very low concentrations where a high noise-to-signal ratio may have contaminated the mass spectra, making them difficult to interpret. A metabolic pathway for the biodegradation of *p*-cresol is proposed (**Appendix 4 (f)**).

#### 4.4.3.3. Bacterial toxicity assessment using *Pseudomonas fluorescens*

The bioluminescence intensity of *Pseudomonas fluorescens* (*P.f.*) was used to evaluate the bacterial toxicity of *p*-cresol in WD and degraded in RPBBR through continuous and batch systems. *P.f.* bioluminescence intensity was found to be lower ( $2.78 \times 10^6$  counts per second) in WD sample than the control sample (distilled water) ( $11.74 \times 10^6$  second). However, the bioluminescence intensity was higher for treated wastewater in CS ( $5.4 \times 10^6$  counts per second) and BS ( $4.2 \times 10^6$  per second) systems than WD sample (**Appendix 4 (g)**). This leads to more mineralization of *p*-cresol in a continuous system. A similar phenomenon was observed under long time exposure (24 h, chronic effects) to degrade *p*-cresol in continuous and batch system (**Appendix 4 (h)**). The WD *p*-cresol sample exhibited  $76.66 \pm 1.8\%$  and  $86.82 \pm 1.62\%$  *P.f.* bioluminescence intensity during acute and chronic toxicities, respectively (**Appendix 4 (g), (h)**). *P.f.* bioluminescence intensity in the continuous system for acute and chronic exposure was obtained to be  $53.66 \pm 1.2\%$  and  $59.47 \pm 1.3\%$ , respectively. Similarly, the *P.f.* bioluminescence intensity for *p*-cresol degraded in the batch system for acute and chronic exposure was found to be  $63.54 \pm 2.32\%$  and  $67.78 \pm 2.15\%$ , respectively (**Appendix 4 (i)**).

#### 4.5. Conclusions

The effect of inoculum, pH, and NaCl% on specific growth was studied to achieve the maximum degradation of *p*-cresol from waste water. The maximum efficiency of  $99.36 \pm 0.2\%$  was obtained at  $100 \text{ mg L}^{-1}$  of initial *p*-cresol concentration. Biodegradation of *p*-cresol followed the first-order kinetics. The performance of RPBBR was adversely affected under high shock-loading rate. During the biodegradation of *p*-cresol, the intermediates identified as maleic acid, glycerol, and 4-methyl catechol. Bacterial toxicity assessment ensures the mineralization of *p*-cresol. RPPBR may be explored further in the secondary stage of wastewater treatment plants (i.e., biological processes) to treat a wide range of pollutants.

